Dazl determines primordial follicle formation through the translational regulation of Tex14

THE FASEB JOURNAL • RESEARCH • www.fasebj.org

Dazl determines primordial follicle formation through the translational regulation of Tex14

Roseanne Rosario,[*,1] James H. Crichton,[†] Hazel L. Stewart,[*] Andrew J. Childs,[‡] Ian R. Adams,[†] and Richard A. Anderson[*]

[*]Medical Research Council (MRC) Centre for Reproductive Health, Queens Medical Research Institute, University of Edinburgh, Edinburgh, United Kingdom; [†]MRC Human Genetics Unit, MRC Institute of Genetics and Molecular Medicine, Western General Hospital, Edinburgh, United Kingdom; and [‡]Department of Surgery and Cancer, Institute of Reproductive and Developmental Biology, Faculty of Medicine, Imperial College London, London, United Kingdom

ABSTRACT: Deleted in azoospermia-like (DAZL) is a germ cell RNA-binding protein that is essential for entry and progression through meiosis. The phenotype of the Dazl knockout mouse has extensive germ cell loss because of incomplete meiosis. We have created a Dazl hypomorph model using short interfering RNA knockdown in mouse fetal ovary cultures, allowing investigation of Dazl function in germ cell maturation. Dazl hypomorph ovaries had a phenotype of impaired germ cell nest breakdown with a 66% reduction in total follicle number and an increase in the proportion of primordial follicles (PMFs), with smaller oocytes within these follicles. There was no significant early germ cell loss or meiotic delay. Immunostaining of intercellular bridge component testis-expressed protein (Tex)14 showed ~59% reduction in foci number and size, without any change in Tex14 mRNA levels. TEX14 expression was also confirmed in the human fetal ovary across gestation. Using 3′UTR-luciferase reporter assays, translational regulation of TEX14 was demonstrated to be DAZL-dependant. Dazl is therefore essential for normal intercellular bridges within germ cell nests and their timely breakdown, with a major impact on subsequent assembly of PMFs.—Rosario, R., Crichton, J. H., Stewart, H. L., Childs, A. J., Adams, I. R., Anderson, R. A. Dazl determines primordial follicle formation through the translational regulation of Tex14. FASEB J. 33, 000–000 (2019). www.fasebj.org

KEY WORDS: germ cell maturation · intercellular bridge · siRNA knockdown · fetal ovary culture

The oocytes in primordial follicles (PMFs) are thought to represent the entire pool of potential gametes available to a female throughout her life. PMFs are assembled during fetal life in humans and early postnatal life in rodents *via* a series of interconnected processes beginning with the migration of primordial germ cells into the gonadal ridge, a process already underway in the human embryo at 4 wk of development (1), and which takes place in mice between embryonic day (e)8.5 and 10.5 (2). The germ cells then expand rapidly in number through mitotic divisions with incomplete cytokinesis, producing a surplus of oogonia linked by intercellular bridges, thus forming what are termed germline cysts or germ cell nests (3). The germ cell nest is an evolutionary conserved structure found in males and females of species ranging from higher insects to frogs, rodent, and other vertebrates (4). It is believed that these nests help increase the store of organelles and nutrients that are later required by the oocyte, an idea that is supported by oocyte development in *Drosophila* (5), where all but one of the cells in the nest become nurse cells that contribute materials to one oocyte (6). Mouse germ cells have also been shown to receive organelles from neighboring cyst cells (7), and it has been proposed that this organelle transport plays an evolutionarily conserved role in mammalian oocyte differentiation (8).

Intercellular bridges have also been hypothesized to play an essential role in the synchronization of the meiotic cycle, as germ cells commence meiosis I while in the nest structure (9). Germ cells progress through the initial stages of prophase of meiosis I before arresting at diplotene, at which point the germ cell nest undergoes breakdown. Nest breakdown is a coordinated effort that involves the loss of germ cells through caspase-dependant apoptosis

ABBREVIATIONS: BOLL, Bol-like; DAZL, deleted in azoospermia-like; HEK, human embryonic kidney; PMF, primordial follicle; PRIM, primary follicle; siRNA, short interfering RNA; Sycp3, synaptonemal complex protein 3; Tex, testis-expressed protein; Tra98, germ cell-specific antigen; TRN, transitionary follicle; wga, week gestational age

[1] Correspondence: MRC Centre for Reproductive Health, University of Edinburgh, 47 Little France Crescent, Edinburgh EH16 4TJ, United Kingdom. E-mail: roseanne.rosario@ed.ac.uk

doi: 10.1096/fj.201901247R
This article includes supplemental data. Please visit *http://www.fasebj.org* to obtain this information.

and physical invasion of the nests by pregranulosa somatic cells (6). During this process, the cytoplasmic bridges between remaining germ cells are either retracted or cleaved, possibly through protease action by the surrounding somatic cells. This culling of excess germ cells may represent a means of selection, through which deficient nuclei are lost and only the highest quality oocytes are assembled into PMFs from mid gestation in humans (10) and at the time of birth in mice (7).

Deleted in azoospermia-like (DAZL) and its homologs DAZ and Bol-like (BOLL) belong to the DAZ family of RNA-binding proteins, which are found almost exclusively in germ cells. DAZL is well established as having an essential role in gametogenesis because targeted disruption of Dazl in mice results in infertility in both males and females (11, 12). Deletion of Dazl causes loss of germ cells in the gonads of both sexes, with increased apoptosis, reduced expression of germ cell markers, and aberrant chromatin structure (11, 13, 14). Germ cells are also unable to induce the expression of meiotic genes in response to retinoic acid (13), and those cells that do enter meiosis are unable to transition from leptotene to zygotene of prophase I as complete synaptonemal complexes fail to form (12). $Dazl^{+/-}$ mice have no germ cell loss up to e16.5 (15) and no differences in follicle number or stage at postnatal d 21 (16), though germ cells and follicles have not been investigated between these timepoints. Dazl has also been shown to have a role in later development during the oocyte-to-zygote transition (17); although, recent data demonstrate that MII oocytes derived from postnatal Dazl conditional knockouts do not have abnormal spindle morphology, suggesting Dazl is not required for fertilization (18). As an RNA-binding protein, DAZL has been shown to bind actively translating polysomes (19) and stimulate the translation of bound mRNA targets (20). Three direct mRNA targets of Dazl characterized in mice are synaptonemal complex protein 3 (*Sycp3*), mouse vasa homolog, and testis-expressed protein (*Tex*)*19.1* (17, 21, 22), whereas ten-eleven translocation methylcytosine dioxygenase 1 has also been demonstrated to be dependent on Dazl for its translation in mouse embryonic stem cells (23). We have used RNA immunoprecipitation and sequencing to identify novel DAZL targets in the human fetal ovary and confirmed the role of DAZL in regulating the translation of *SYCP1*, structural maintenance of chromosomes protein 1B, and *TEX11* (24). However, there have been numerous screens for Dazl targets, which have identified potential mRNAs that have not been further validated. One such mRNA is Tex14 (22), which is an essential component of male and female intercellular bridges (25).

Although Dazl has been well studied during early germ cell development, the majority of this work has been carried out using the Dazl knockout mouse, which characteristically loses all germ cells, precluding further analysis. Therefore, we sought to develop a model in which Dazl expression was reduced, but with minimized loss of germ cells, which would enable us to specifically study the role of Dazl in germ cell development. This is potentially significant to human reproduction because polymorphisms in DAZL may influence risk of premature ovarian insufficiency and age at menopause in women (26). Although this finding has not been corroborated in other studies (27, 28), it suggests that hypomorphic polymorphisms and single nucleotide polymorphisms that quantitatively reduce DAZL expression or function in human germ cells may potentially have consequences for fertility and reproductive lifespan in women. We have used our model, which uses short interfering RNA (siRNA), to knockdown Dazl expression in the mouse fetal ovary as meiosis commences, to investigate the role of Dazl once meiosis is underway, and to investigate the impact of Dazl in subsequent PMF formation. With this model, we have demonstrated for the first time that Dazl is important in the formation and breakdown of germ cell nests as well as in subsequent PMF formation *via* the translational regulation of Tex14.

MATERIALS AND METHODS

Collection of human fetal ovaries

Ethical approval for this study was obtained from Lothian Research Ethics Committee, United Kingdom (LREC 08/S1101/1), and women gave informed written consent. Human fetuses [8–20 wk gestational age (wga)] were obtained after elective termination of pregnancy, and all fetuses used in this study were morphologically normal. Gestational age was determined by ultrasound scan and confirmed (for second trimester fetuses) by direct measurement of foot length. The sex of first trimester fetal gonads was determined by PCR for the *SRY* gene (29). Extraovarian tissue was removed from dissected ovaries, which were then fixed in Bouins for 2–3 h before processing into paraffin blocks for immunohistochemical analysis.

Animals

Experiments involving mice were approved by the University of Edinburgh Animal Research Ethics Committee, and performed according to the UK Animal (Scientific Procedures) Act 1986. Wild-type CD-1 mice were maintained and bred in an environmentally controlled room on a 12-h light/dark photoperiod from 7 AM each day and fed *ad libitum* according to the UK Home Office and local University of Edinburgh ethical standards. To obtain fetuses for ovary culture experiments, mouse breeding harems were set up and females checked for the presences of a copulation plug; this was designated as e0.5.

Fetal ovary culture

Pregnant timed-mated females were obtained at e13.5 and culled by cervical dislocation. Fetal ovaries with attached mesonephros were dissected from female embryos; the day of dissection was designated d 0 of culture. Ovary and attached mesonephros were cultured for either 3, 6 or 12 d on a 2% agar block in a 35-mm Petri dish, incubated at 37°C, 5% CO_2. For the first 3 d of culture (d 0–3), culture media contained DMEM (Thermo Fisher Scientific, Waltham, MA, USA) supplemented with 10% fetal bovine serum, 2 mM L-glutamine, 10 μM β-mercaptoethanol, and 1% sodium pyruvate. For subsequent days of culture, media were replaced with a simple culture medium consisting of α-MEM (Thermo Fisher Scientific) supplemented solely with 3 mg/ml bovine serum albumin (BSA). Medium was replaced with fresh every 72 h. To knock down Dazl expression, cultured fetal ovaries were transfected with 15 or 50 nM of Dazl Stealth RNAi siRNA

(Thermo Fisher Scientific) or a GC-matched control using Metafectene Pro (Biontex Laboratories, Munchen, Germany) and Opti-MEM serum free medium (Thermo Fisher Scientific). siRNA-lipid complexes were added to fetal ovaries on d 0 of culture and removed on d 3 of culture when medium was replaced.

RNA extraction, cDNA synthesis, and quantitative RT-PCR

To assess *Dazl* knockdown, cultured mouse fetal ovaries were collected in Trizol (Thermo Fisher Scientific) and homogenized using a motorized pellet pestle, and RNA was extracted according to the manufacturer's instructions. To assess RNA stability after luciferase assays, cytoplasmic RNA from luciferase-transfected human embryonic kidney (HEK)-293T cells was extracted with the Cytoplasmic and Nuclear RNA Purification Kit (Norgen-Biotek, Thorold, ON, Canada) according to the manufacturer's instructions. RNA was reverse transcribed to cDNA using concentrated random primers and Superscript III reverse transcriptase (Thermo Fisher Scientific) according to the manufacturer's instructions, and the cDNA synthesis reaction was diluted appropriately before proceeding. Primers for quantitative RT-PCR were designed to amplify all transcript variants and are exon-spanning. Primer pair efficiencies were calculated with the LinReg PCR applet (30). Each reaction was performed in a final volume of 10 μl, with 1× Brilliant III SYBR Green qPCR Master Mix (Agilent Technologies, Santa Clara, CA, USA), 20 pmol of each primer and 2 μl of diluted cDNA. Primer sequences are as follows written in the 5′ to 3′ direction: *Dazl* forward 5′-TGGACCGAAGCATACAGACA-3′, *Dazl* reverse 5′-ACTGCCCGACTTCTTCTGAA-3′, *Boll* forward – 5′-TGTGTTCCTCCTCCACTGTC-3′, *Boll* reverse - 5′-TCATAGGTGCAGGCATAGCA-3′, *Luciferase* forward - 5′-ATCGTGGTGTGCTCTGAGAA-3′, *Luciferase* reverse - 5′-CACGGTAGGCTGAGAAATGC-3′, *Renilla* forward - 5′-CGAAGAGGGCGAGAAAATGG-3′, *Renilla* reverse - 5′-TCTCCTTGAATGGCTCCAGG-3′, *Tex14* F - 5′-GCCAGAGAGAAGGGAGTCAG-3′, *Tex14* R - 5′-ACGGTCCAGTTCCAATCAGT-3′, see Van den Bergen *et al*. (31) for *MAPK1* and calnexin precursor (*Canx*) sequences. Each cDNA sample was analyzed in triplicate. For expression analyses in cultured mouse fetal ovary, target genes were normalized to the geometric mean expression of *Canx* and *Mapk1* (31). For *Luciferase* expression, the *Renilla* sequence, which was located on the same construct, was used for normalization. Data analysis for relative quantification of gene expression and calculation of SD was performed as outlined (32, 33).

Immunohistochemistry

Single immunostaining for germ cell-specific antigen (Tra98) was used to identify germ cells for counting after Dazl knockdown at d 3 and 6 of culture, and single immunostaining for Tex14 was used to investigate intercellular bridges after Dazl knockdown on d 2 of culture. Single immunostaining for Dazl was also used to quantify Dazl protein expression on d 12 of culture. For these analyses, cultured fetal ovaries were fixed for 2 h in Bouins solution and 3 h in 4% paraformaldehyde, respectively. Double immunostaining for Dazl and Tra98 was used to assess the reduction in Dazl expression in mouse fetal ovaries cultured with siRNA, and for this, ovaries were fixed for 6 h in 4% neutral buffered formalin. Double immunostaining for DAZL and TEX14 was also carried out in human fetal ovarian tissue fixed for 2 h in Bouins. After processing, tissue was sectioned, dewaxed, and rehydrated, and antigen retrieval was carried out in either 0.01 M citrate buffer, pH 6 (Dazl-Tra98 and Tra98) or 10 mM Tris/1 mM EDTA buffer with 0.05% Tween 20, pH 9 (Tex14). Endogenous peroxidase activity was blocked with Dako Real Peroxidase-Blocking solution (Agilent Technologies). Tissues were blocked in PBS containing 5% BSA and 20% normal goat serum and then incubated overnight at 4°C with primary antibodies diluted in blocking serum [Dazl: 1 in 200 (MCA2336; Bio-Rad, Hercules, CA, USA), Tra98: 1 in 200 (Ab82527; Abcam, Cambridge, MA, USA), Tex14: 1 in 100 (18351-1-AP; Proteintech Group, Rosemont, IL, USA), and TEX14 1:4000 (ab154706; Abcam)]. Single immunostaining for Tra98 was carried out using ImmPress reagent (Vector Laboratories, Burlingame, CA, USA) according to the manufacturer's instructions, and slides were counterstained with hematoxylin before mounting. For single Tex14 immunofluorescence, tissues were incubated with an Alexa-conjugated secondary antibody (1:200 dilution) for 1 h at room temperature and counterstained with DAPI before mounting. For double immunofluorescence, tissues were incubated with a peroxidase-conjugated antibody for 30 mins at room temperature before visualization using tyramide signal amplification (PerkinElmer, Waltham, MA) according to the manufacturer's instruction. The first primary antibody (Dazl or TEX14) was then removed by a second antigen retrieval performed by microwaving slides in boiling 0.01 M citrate buffer for 2.5 min. After cooling, slides were blocked as before and incubated overnight at 4°C with anti-rat Tra98 (1:400) or anti-DAZL (1:200, MCA2336; Bio-Rad). Secondary antibody and visualization steps were carried out as above, before counterstaining with DAPI and mounting. Images were captured using an Axioscan slide scanner (Carl Zeiss GmbH, Oberkochen, Germany) and a 710 confocal microscope (Carl Zeiss) and Zen 2009 software. Relative pixel intensities were quantified using Fiji software according to the manufacturer's instructions (National Institutes of Health, Bethesda, MD, USA; *https://imagej.net/Fiji*). To quantify Dazl knockdown on d 3 of culture, Dazl pixel intensities were normalized to Tra98 pixel intensities. To quantify Dazl knockdown on d 12 of culture, Dazl pixel intensities were normalized to germ cell number, as there is no reliable marker that labels all germ cells at this time point.

Chromosome spreads and immunostaining

Ovaries were taken at d 5 of culture and oocyte chromosome spreads were prepared as previously described in Peters *et al*. (34). For immunostaining, slides were first washed in PBS, then blocked in PBS containing 0.15% BSA, 0.1% Tween-20, and 5% goat serum. Slides were then incubated with mouse anti-Sycp3 (1:500, ab97672; Abcam) and either rabbit anti-Sycp1 (1:200, ab15090; Abcam) or guinea pig anti-Sycp1 (1:200; Howard Cooke Laboratory, Edinburgh, United Kingdom) primary antibodies, diluted in block buffer. Alexa Fluor–conjugated secondary antibodies (Thermo Fisher Scientific) were used at a 1:500 dilution, and 2 ng/μl DAPI was used to fluorescently stain DNA. Slides were mounted in 90% glycerol, 10% PBS, 0.1% p-phenylenediamine. Images were captured using a Photometrics Coolsnap HQ2 CCD or Photometric Prime BSI camera and a Zeiss AxioImager A2 fluorescence microscope with Plan-neofluar objectives (Carl Zeiss, Cambridge, United Kingdom). Image capture was performed using Micromanager (*https://open-imaging.com/*).

Meiotic staging

Oocytes were substaged based on synaptonemal complex formation-dissolution using staining patterns of the axial element protein Sycp3, which marks the axis of each homolog, and the transverse filament protein Sycp1, which marks the regions of chromosome synapsis. All Sycp3-positive oocytes were scored. Pachytene oocytes contain at least 1 fully synapsed pair of homologous chromosomes. As synapsis is not synchronous, some homologs occasionally have partially separate axes. In early diplotene, homologous chromosomes are beginning to desynapse and have intact elongated axial elements, but

limited synapsis, and no completely synapsed homologous. Synaptonemal complex disassembly is apparent in late-diplotene as axial elements become short and fragmented, with little or no synapsis.

Germ cell counts and histologic follicle assessment

Fetal ovaries were fixed for 2 h in Bouins solution on d 3, 6, and 12 of culture, paraffin wax-embedded, sectioned, and stained for Tra98 (germ cell marker) or with hematoxylin and eosin. Assessment of germ cell number was carried out on every sixth section with the Abercrombie correction factor being applied to raw counts to estimate total germ cell number per ovary (35). For d 12 cultured tissue, germ cells were counted as the sum of all oocytes in follicles and all oocytes in nests. Assessment of follicle stage and health was carried out (blinded) on every sixth section of d 12 cultured tissue. A follicle was counted only where the analyzed section contained an oocyte with a visible germinal vesicle. PMFs were defined as having only squamous pregranulosa cells; transitionary follicles (TRNs) were considered to have both squamous and cuboidal granulosa cells; and primary follicles (PRIMs) had a complete layer of cuboidal granulosa cells. Follicle health was assessed as previously described in Stefansdottir *et al*. (36). The Abercrombie correction factor was applied to raw counts to estimate total follicle number per ovary (35).

RNA immunoprecipitation and sequencing

RNA immunoprecipitation for DAZL and sequencing was carried out as outlined in Rosario *et al*. (24). The raw data are available at Gene Expression Omnibus (GEO) using the study ID: GSE81524. The dataset was reanalyzed with thresholds of false discovery rate <0.001 and log-fold change >2.

Cloning

The R115G mutant DAZL overexpression construct was cloned as previously described in ref. (24). The TEX14 3′UTR-luciferase construct was cloned by subcloning the TEX14 3′UTR sequence from a pLightSwitch 3′UTR clone and inserting this into pEZX-MT06 (referred to as 3′UTR-luciferase empty vector control) using *Eco*RI and *Xho*I.

Luciferase assay

HEK293T cells were cultured in DMEM + GlutaMAX supplemented with 10% fetal bovine serum and maintained at 37°C in 5% CO_2. For the luciferase assays, cells were seeded at a density of 20,000 cells per well of a 96-well plate. Cells were transfected with 10 ng of the 3′UTR-luciferase construct (TEX14 or glyceraldehyde 3-phosphate dehydrogenase) or a 3′UTR-luciferase empty vector control (Genecopoeia, Rockville, MD, USA), plus 100 ng of either a wild-type DAZL overexpression construct, a R115G mutant DAZL overexpression construct, or a vector-only control (OriGene Technologies, Rockville, MD, USA), using Lipofectamine 3000 Transfection Reagent (Thermo Fisher Scientific). Luciferase expression was detected 48 h after transfection using the Dual-Glo Luciferase Assay System according to the manufacturer's instructions.

Statistical analysis

All data are shown as means ± SE of the mean and were analyzed using Prism 7 software (GraphPad Software, La Jolla, CA). Mann-Whitney (unpaired data) and Wilcoxon test (paired data) statistics were carried out as appropriate. The Friedman test was used to calculate statistical significance of 3′UTR-luciferase reporter assays. A value of $P < 0.05$ was considered statistically significant.

RESULTS

Dazl mRNA and protein expression are reduced in fetal ovaries cultured for 3 d with siRNA

Dazl knockout mouse ovaries lack follicular structures because germ cells are unable to transition from the leptotene to zygotene stage of prophase I, and consequently undergo apoptosis at ~e17.5 (11, 12); however, this apoptosis can be observed as early as e14.5 in an inbred line of mice (13, 37). We therefore used siRNA technology to create a Dazl hypomorph model in order to study the effects of reduced Dazl expression on meiotic progression and subsequent PMF formation. Three different siRNAs were initially tested for efficiency of Dazl knockdown before 1 was chosen (Supplemental Fig. S1). To validate this model, Dazl mRNA levels and protein expression were analyzed in mouse fetal ovaries cultured for 3 d with siRNA (**Fig. 1**). Two doses of siRNA (15 and 50 nM) were tested and resulted in ~60 and 75% reduction in Dazl mRNA levels, respectively, when compared with ovaries cultured with a scramble siRNA (Fig. 1*A–D*) (both $P = 0.028$). Importantly, this treatment did not result in any change in the RNA expression of the closely related RNA-binding protein Boll (Supplemental Fig. S2). Given difficulties in ascertaining Dazl protein in mouse fetal tissue by Western blotting (16), immunostaining for Dazl was performed on tissue cultured for 3 d with both concentrations of siRNA, and pixel intensity was quantified to estimate the change in protein (Fig. 1*B–E*). This was normalized to immunostaining for the germ cell marker Tra98 to ensure changes observed in Dazl expression were not caused by a loss of germ cells. Using this quantification method, there was ~40 and 60% decrease in Dazl protein expression relative to ovaries cultured with scramble siRNA at 15 and 50 nM siRNA doses, respectively (Fig. 1*C–F*) [$P = 0.002$ (15 nM dose), $P = 0.05$ (50 nM dose)]. Both concentrations of siRNA were used in subsequent experiments.

Knockdown of Dazl does not cause early loss of germ cells

We sought to investigate whether knockdown of Dazl causes a loss in germ cell number, a phenotype which is seen in the Dazl null mouse. To do this immunostaining for the germ cell marker Tra98 was utilized and germ cell counts were performed on d 3, 6, and 12 of culture. On d 12 of culture, the number of oocytes found in follicles as well the number of germ cells observed in nests were combined to give a total germ cell count. There was no significant difference in total germ cell number per ovary between scramble siRNA–cultured and Dazl siRNA–cultured

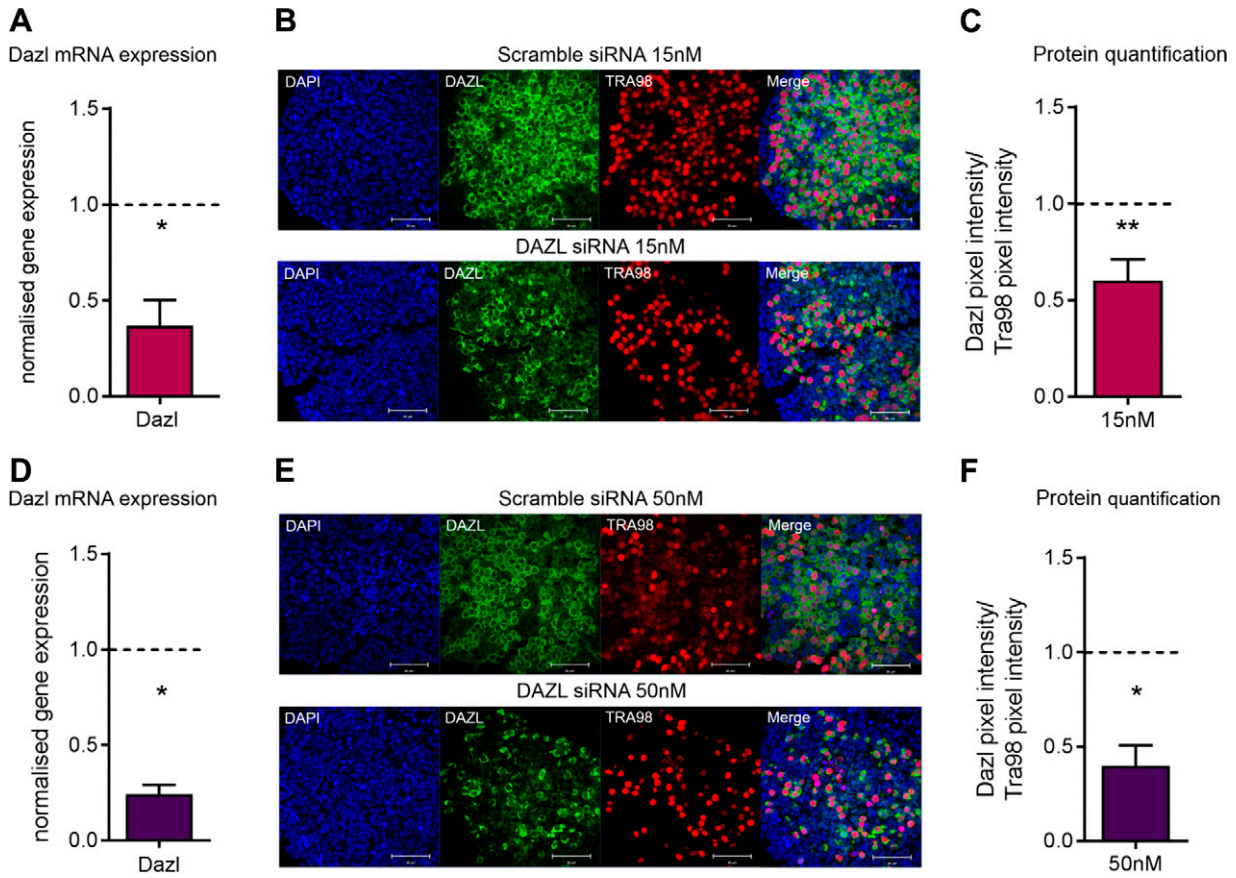

Figure 1. Validation of Dazl knockdown in e13.5 cultured ovaries using 15 and 50 nM of siRNA. *A*) Dazl mRNA expression in Dazl hypomorph ovaries relative to scramble-control ovaries cultured with 15 nM of siRNA. Expression was analyzed 3 d after transfection. Graph displays means of $n = 4$ ovaries for each group. Expression in scramble-control ovaries depicted by dashed line. Error bars indicate means ± SE. $P = 0.028$, Mann-Whitney. *B*) Representative image of immunostaining for Dazl (green) and Tra98 (red) in Dazl hypomorph and scramble-control ovaries cultured with 15 nM of siRNA. Immunostaining was performed 3 d after transfection. Scale bars, 50 μM. *C*) Quantification of Dazl and Tra98 immunostaining in Dazl hypomorph and scramble-control ovaries cultured with 15 nM of siRNA. Graph displays mean of Dazl immunostaining pixel-intensity relative to Tra98 immunostaining pixel-intensity relative. Error bars indicate means ± SE; $n = 4$ ovaries for each group. $P = 0.002$, Mann-Whitney. *D*) Dazl mRNA expression in Dazl hypomorph ovaries relative to scramble-control ovaries cultured with 50 nM of siRNA. Expression was analyzed 3 d after transfection. Graph displays means of $n = 4$ ovaries for each group. Expression in scramble-control ovaries depicted by dashed line. Error bars indicate means ± SE. $P = 0.028$, Mann-Whitney. *E*) Representative image of immunostaining for Dazl (green) and Tra98 (red) in Dazl hypomorph and scramble-control ovaries cultured with 50 nM of siRNA. Immunostaining was performed 3 d after transfection. Scale bars, 50 μM. *F*) Quantification of Dazl and Tra98 immunostaining in Dazl hypomorph and scramble-control ovaries cultured with 50 nM of siRNA. Graph displays mean of Dazl immunostaining pixel-intensity relative to Tra98 immunostaining pixel-intensity relative. Error bars indicate means ± SE; $n = 4$ ovaries/group. $P = 0.05$, Mann-Whitney.

ovaries on d 3 and 6 of culture (**Fig. 2**). However, there was a small decrease in germ cell number on d 12 of cultures, and this was significant in the 50 nM dose culture (466 ± 33 *vs.* 344 ± 27; $P = 0.03$), potentially suggesting low levels of apoptosis occurring around the time of nest breakdown and follicle formation in these cultures.

PMF formation is delayed following knockdown of Dazl

The e13.5 fetal mouse ovary culture system in which we have knocked down Dazl can be extended up to 12 d, thus spanning from the onset of meiosis in germ cells to the formation of PMFs and the subsequent initiation of growth in some follicles. In keeping with the transient nature of siRNA transfection, there was no difference in Dazl protein expression between scramble siRNA–cultured and Dazl siRNA–cultured ovaries. In Dazl hypomorph ovaries treated with the 15 nM dose, Dazl protein expression was 108 ± 19% ($n = 3$) compared with scramble siRNA–treated ovaries, and 98 ± 14% ($n = 5$) with the 50 nM dose. At d 12 of culture, the total number of follicles present in Dazl and scramble siRNA–treated ovaries was assessed, and follicles were staged as primordial, transitionary, or primary. Ovaries cultured with Dazl siRNA (for the first 3 d of culture) had significantly fewer follicles compared with scramble siRNA–cultured ovaries (**Fig. 3*A*, *B***); this decrease was evident at both doses of siRNA and more pronounced at 50 nM where there was ~50% reduction in the total number of follicles ($P = 0.016$). In addition to having a reduced number of follicles, Dazl hypomorph

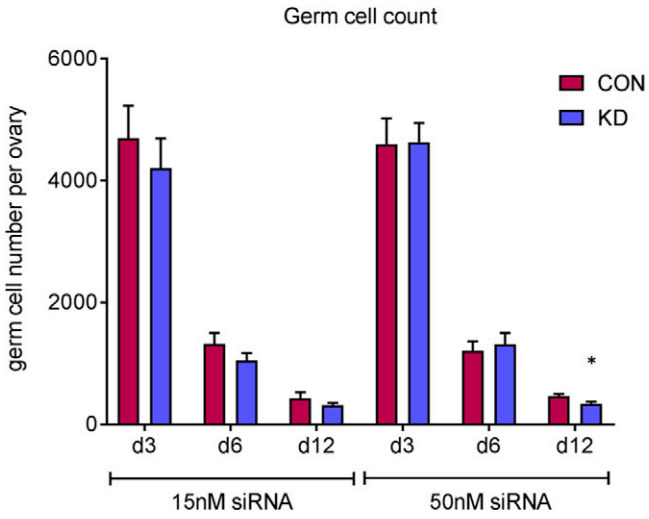

Figure 2. Germ cell number at d 3, 6, and 12 of culture in e13.5 cultured ovaries using 15 and 50 nM of siRNA. Germ cell number was quantified at d 3, 6, and 12 of culture in scramble-control and Dazl hypomorph ovaries. CON, control; KD, knockdown. Error bars indicate means ± SE; n = 6–8 ovaries/group. P = 0.03, Wilcoxon test.

ovaries had proportionally more PMFs than growing follicles (transitional and PRIMs) compared with scramble control–cultured ovaries (Fig. 3*C, D*) ($P < 0.001$). Furthermore, the PMFs in Dazl hypomorph ovaries had a significantly smaller oocyte diameter than PMFs in scramble control–cultured ovaries at both siRNA doses (Fig. 3*E*). These PMFs remained consistently smaller even after culture up to 14 d (Fig. 3*F*). The Dazl hypomorph model also contained a significant number of oocytes within germ cell nest structures (P = 0.016, Fig. 3*G*), which had not broken down to form PMFs. Taken together, these data suggest that the knockdown of Dazl in the fetal mouse ovary impacts the breakdown of germ cell nests and the assembly of PMFs, causing a reduction in the total number of follicles formed.

Knockdown of Dazl does not delay meiotic progression

As Dazl targets RNA from many key meiotic genes (38) and Dazl knockout oocytes are unable to progress through meiotic prophase (12, 13), we investigated whether defective meiotic progression could be responsible for follicle reduction in the Dazl knockdown ovaries. Oocyte chromosome spreads were prepared from ovaries on d 5 of culture to capture oocytes in late meiotic prophase I, and stained with antibodies against components of the synaptonemal complex to substage oocytes: axial element protein Sycp3 and transverse filament protein Sycp1. A total of 125 oocytes from ovaries treated with scramble siRNA and 166 from Dazl siRNA–treated ovaries were analyzed. Oocytes from 3 stages were identified: firstly pachytene, with overlapping extended filaments of Sycp3 and Sycp1 identifying fully synapsed homologous chromosomes; secondly, early diplotene, with intact Sycp3 filaments undergoing homologous chromosome desynapsis and only colocalizing with limited filaments of Sycp1; and finally, late-diplotene and dictyate, with fragmented Sycp3 filaments and little or no overlapping Sycp1 (**Fig. 4*A***).

From 15 nM scramble siRNA–cultured ovaries, on average, 75 ± 6.5% of oocytes were in pachytene, 12 ± 2.1% in early diplotene, and 13 ± 5.8% in late-diplotene and dictyate (Fig. 4*B*). Representation of the different substages was unaltered in 15 nM Dazl hypomorph ovaries, with an average of 73 ± 11.7% in pachytene, 12 ± 3.4% in early diplotene, and 15 ± 8.5% in late-diplotene and dictyate (Fig. 4*B*). Oocytes were also analyzed following 50 nM siRNA culture to investigate whether a stronger knockdown of Dazl affected meiotic progression. In 50 nM scramble siRNA–cultured ovaries, on average, 54 ± 5.2% of oocytes were in pachytene, 21 ± 2.6% in early diplotene, and 25 ± 5.3% in late-diplotene and dictyate (Fig. 4*C*). Again, despite the increased Dazl knockdown, no difference in meiotic progression was detected in 50 nM Dazl hypomorph oocytes, of which an average of 44 ± 4.9% were in pachytene, 23 ± 2.9% in early diplotene, and 32 ± 4.0% are in late-diplotene and dictyate (Fig. 4*C*). Therefore, progression of oocytes through meiotic prophase I is not detectably perturbed in response to Dazl knockdown.

Dazl knockdown interferes with germ cell nest breakdown *via* Tex14

Because many germ cells were still found in nest structures on d 12 of culture and had not formed PMFs in Dazl hypomorph ovaries, we investigated whether germ cell nest breakdown was affected through assessment of Tex14 expression, because Tex14 is an essential component of male and female intercellular bridges (25). Tex14 expression was analyzed using immunofluorescence on d 2 of culture (48 h after transfection) because germ cell nests have already been formed and Tex14 expression is at its highest. There was a striking difference in Tex14 expression between scramble siRNA and Dazl hypomorph ovaries (**Fig. 5*A***), with a significant decrease in the number of Tex14 foci in Dazl hypomorph ovaries (P = 0.029). Additionally, these foci were significantly smaller than those in scramble siRNA–cultured ovaries (P = 0.029) (Fig. 5*B, C*). As Dazl is an RNA-binding protein and a known regulator of mRNA stability and translation, Tex14 mRNA levels were quantified at this time point to see if there were similar changes to those observed in Tex14 protein expression. However, there were no differences in Tex14 mRNA levels in Dazl hypomorph ovaries relative to scramble siRNA ovaries (Fig. 3*D*). This suggests that the reduction in Tex14 protein may indicate translational regulation of Tex14 mRNA by Dazl.

DAZL and TEX14 are coexpressed across gestation in the human fetal ovary

Although *TEX14* transcripts have been studied across gestation in the human fetal ovary (39), TEX14 expression

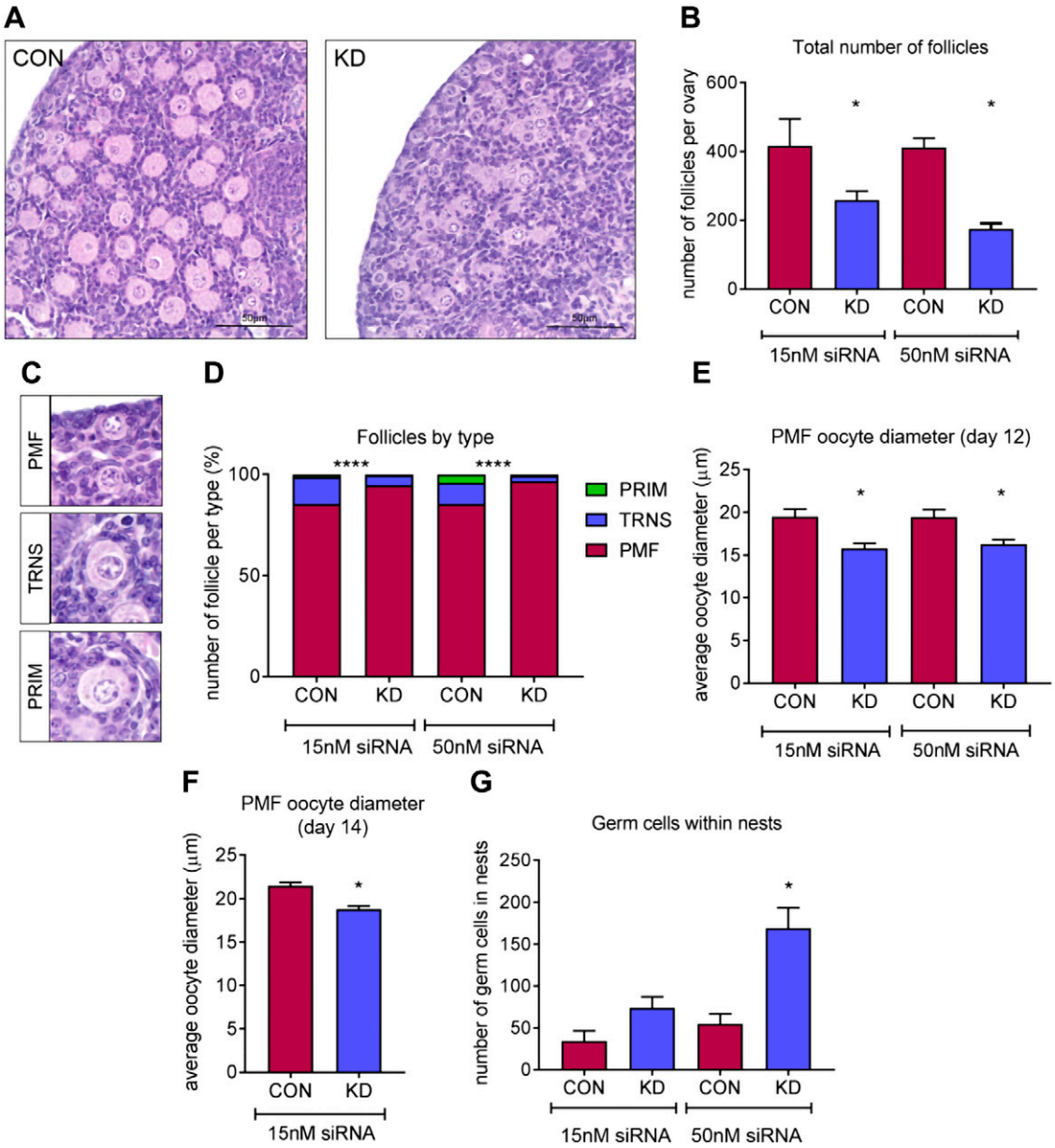

Figure 3. Assessment of follicles after 12 d of culture in e13.5 cultured ovaries using 15 and 50 nM of siRNA. *A*) Representative hematoxylin and eosin images from Dazl hypomorph and scramble-control siRNA ovaries cultured for 12 d. Scale bar, 50 μM. *B*) Graph depicts total number of follicles in Dazl hypomorph and scramble-control ovaries cultured for 12 d with 15 and 50 nM of siRNA for the first 3 d of culture. Error bars indicate means ± SE; $n = 7$–8 ovaries/group. $P = 0.0234$ (15 nM dose); $P = 0.016$ (50 nM dose), Wilcoxon test. *C*) Representative hematoxylin and eosin images of PMFs, TRNs, and PRIMs; PMFs were defined as having only squamous pregranulosa cells, TRNs were considered to have both squamous and cuboidal granulosa cells, and PRIMs had a complete layer of cuboidal granulosa cells. *D*) Graph depicts the proportion of follicles staged as PMF, TRN, or PRIM in Dazl hypomorph and scramble-control ovaries cultured for 12 d with 15 and 50 nM of siRNA for the first 3 d of culture; $n = 7$–8 ovaries/group, $P < 0.0001$, χ^2 test. *E*) Graph depicts PMF diameter in oocytes from Dazl hypomorph and scramble-control cultured ovaries. Ovaries were cultured for 12 d with siRNA for the first 3 d. All PMFs were measured in each ovary. Error bars indicate means ± SE; $n = 5$. $P = 0.01$ (15 nM); $P = 0.0238$ (50 nM), Wilcoxon test. *F*) Graph depicts PMF diameter in oocytes from Dazl hypomorph and scramble control –cultured ovaries. Ovaries were cultured for 14 d with 15 nM dose of siRNA for the first 3 d. A total of 75 PMFs were measured from 2 Dazl hypomorph and scramble-control ovaries. Error bars indicate means ± SE; $n = 2$. $P < 0.0001$, Wilcoxon test. *G*) Graph depicts number of germ cells found in nest structures in Dazl or scramble-control siRNA ovaries after 12 d of culture. All germ cells found in nests in each ovary were counted. Con, control; KD, knockdown. Error bars indicate means ± SE; $n = 7$–8 ovaries/group. $P = 0.016$, Wilcoxon test.

has not been previously characterized. Expression of DAZL and TEX14 was assessed in the human fetal ovary across gestation (**Fig. 6**), which included germ cells at the initiation of meiosis (13–16 wga) and later in meiosis including onset of meiotic arrest and PMF formation (18 wga). As previously described in ref. (40), DAZL expression was observed in the cytoplasm of germ cells, and this expression was similar between 13 wga and 16 wga specimens; DAZL expression decreased by 18 wga. At all gestations examined, the

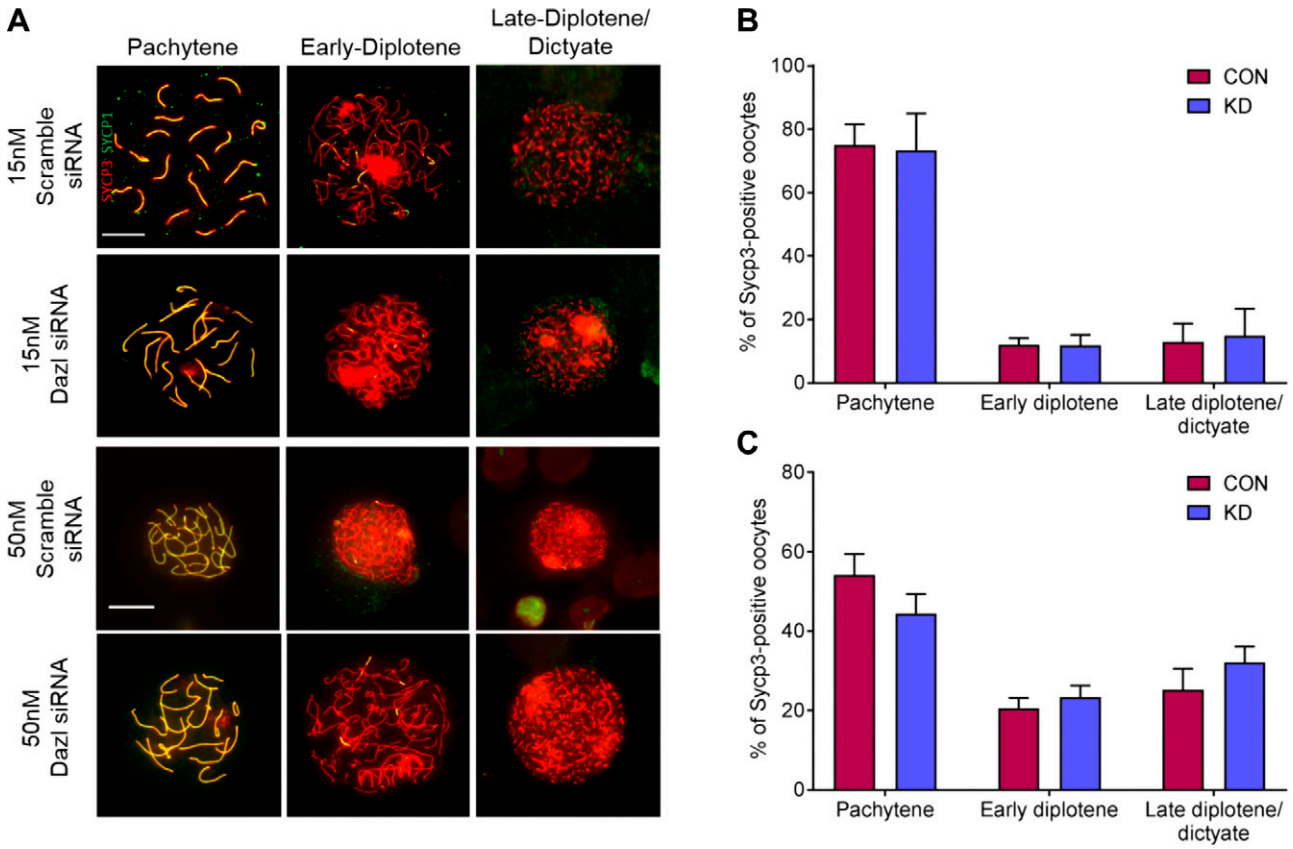

Figure 4. Substaging meiotic prophase I oocytes from e13.5 cultured ovaries using 15 and 50 nM of siRNA. *A*) Immunostaining of Sycp3 (red) and Sycp1 (green) to assess axial element and transverse filament formation, respectively. Representative merged images displayed. Scale bars, 10 μm, are consistent across 15 and 50 nM culture images. *B*) Relative proportions of pachytene, early diplotene, and late-diplotene and dictyate oocytes from d 5 cultured ovaries following 15 nM siRNA treatment. Bar graphs display mean percentages from 3 repeats, and a total of 125 scramble siRNA, and 166 Dazl siRNA–cultured oocytes. *C*) Relative proportions of pachytene, early diplotene, and late-diplotene and dictyate oocytes from d 5 cultured ovaries following 50 nM siRNA treatment. Bar graphs display mean percentages from 3 repeats, and a total of 291 scramble siRNA, and 287 Dazl siRNA–cultured oocytes. Con, control; KD, knockdown. Error bars indicate means ± SE.

majority of TEX14 foci were observed in the cytoplasm of DAZL-positive germ cells that were interconnected in germ cell nest structures.

DAZL binds the 3′UTR of TEX14 and stimulates translation

DAZL RNA immunoprecipitation and sequencing was previously carried out using human fetal ovarian tissue (24). Using thresholds of false discovery rate <0.001 and log-fold change >2, these data showed that TEX14 expression was significantly enriched as a result of DAZL immunoprecipitation compared with a control IgG immunoprecipitation (**Fig. 7*A***). A 3′UTR-luciferase reporter assay in HEK293T cells was used to investigate the possible role of DAZL on TEX14 translation. The presence of DAZL resulted in a 2-fold increase in TEX14 luciferase activity compared with the vector-only control (Fig. 7*B*; $P = 0.027$). No stimulation of translation was observed with a glyceraldehyde 3-phosphate dehydrogenase 3′UTR or in the absence of a 3′UTR, indicating this effect of DAZL is specific to the TEX14 3′UTR. The DAZL R115G mutation was identified in a woman with spontaneous premature ovarian failure (41) and has an impaired ability to bind RNA because the mutation is located within the DAZL RNA recognition motif (42). Expression of the R115G mutant in HEK293T cells resulted in no significant increase in luciferase activity compared with the vector-only control for any of the 3′UTRs assessed. This indicates that the effect of DAZL on TEX14 translation is dependent on its RNA-binding ability. As mRNA translation and mRNA stability are often linked, we examined the steady-state levels of cytoplasmic *luciferase* mRNA to determine whether the changes in TEX14 luciferase activity (Fig. 7*B*) were a consequence of altered *luciferase* mRNA stability. There was no significant difference in *luciferase* mRNA level with DAZL expression, indicating a specific effect on translation (Fig. 7*C*).

DISCUSSION

Given its role as a key determinant of germ cell maturation and entry to meiosis, the germ cell-specific RNA-binding protein Dazl is often referred to as a "germ cell master regulator" (11). It acts at least in part as a "competence factor," permitting responsiveness to somatic cues,

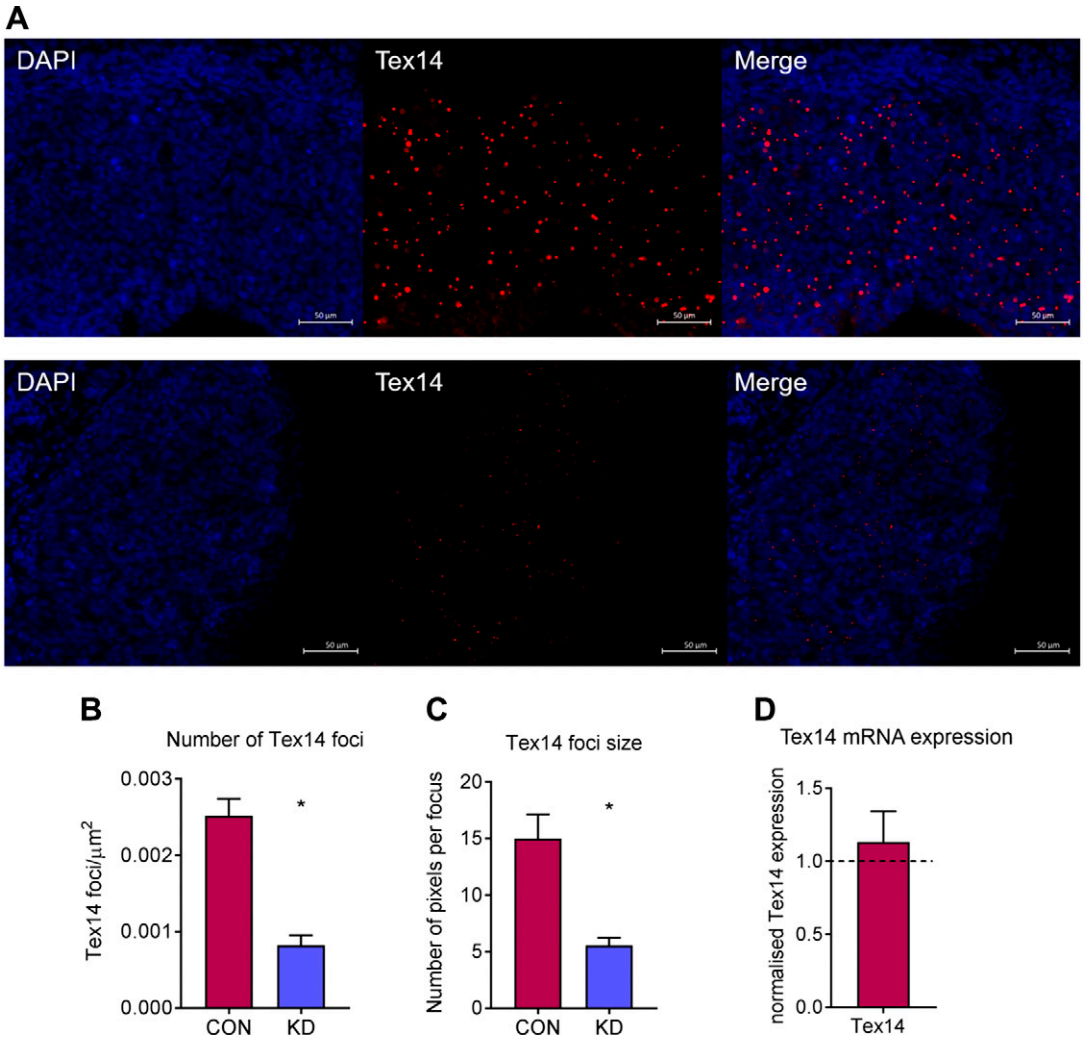

Figure 5. Assessment of intercellular bridge formation at d 2 of culture in e13.5 cultured ovaries using 50 nM of siRNA. *A*) Representative images of Tex14 immunostaining in scramble-control and Dazl hypomorph ovaries cultured with 50 nM of siRNA. Scale bars, 50 μM. *B*) Quantification of Tex14 foci in scramble-control and Dazl hypomorph ovaries. Graph displays total number of foci relative to the area of the ovary. Error bars indicate means ± SE; $n = 4$ ovaries/group. $P = 0.029$, Mann-Whitney. *C*) Quantification of Tex14 focus size in scramble-control and Dazl hypomorph ovaries. Graph displays the number of pixels per Tex14 focus. Error bars indicate means ± SE; $n = 4$ ovaries/group. $P = 0.029$, Mann-Whitney. *D*) Tex14 mRNA expression in Dazl hypomorph ovaries relative to scramble-control ovaries. Expression was analyzed 3 d after transfection. Con, control; KD, knockdown. Graph displays means of $n = 4$ ovaries for each group. Expression in scramble-control ovaries depicted by dashed line. Error bars indicate means ± SE.

specifically retinoic acid, at entry to meiosis (43). Although the phenotype of Dazl deficiency in both sexes demonstrates its obligate significance for fertility, the loss of germ cells shortly after the initiation of meiosis in the knockout mouse model prevents analysis of the role of Dazl in later germ cell maturation. To address this, we have established a Dazl hypomorph model where siRNA is used to reduce, but not completely silence, Dazl expression at the onset of meiosis, and there is no significant loss of germ cells. With this model we have demonstrated that knockdown of Dazl expression had a significant impact on the formation of the ovarian reserve because it interfered with the breakdown of germ cell nests and subsequent PMF assembly. We suggest that this is potentially a consequence of abnormal translational regulation of Tex14, which we have shown for the first time to be a DAZL mRNA target.

This e13.5 fetal mouse ovary culture technique supports survival of premeiotic germ cells, progression through prophase I of meiosis up to diplotene arrest, followed by PMF formation and subsequent growth initiation (36). Therefore, this culture system spans both fetal and neonatal stages of germ cell development, allowing us to examine the role of Dazl across a range of stages of germ cell maturation *in vitro*. We observed that Dazl hypomorph ovaries had significantly fewer follicles than scramble-control ovaries. Initially, the most obvious explanation for this was that the knockdown of Dazl caused loss of germ cells in our culture model. However, there were no significant differences in germ cell number between Dazl knockdown and scramble-control ovaries at d 3 and 6 of culture with either dose of siRNA. A small reduction was seen at d 12 of culture, which was significant with the higher dose

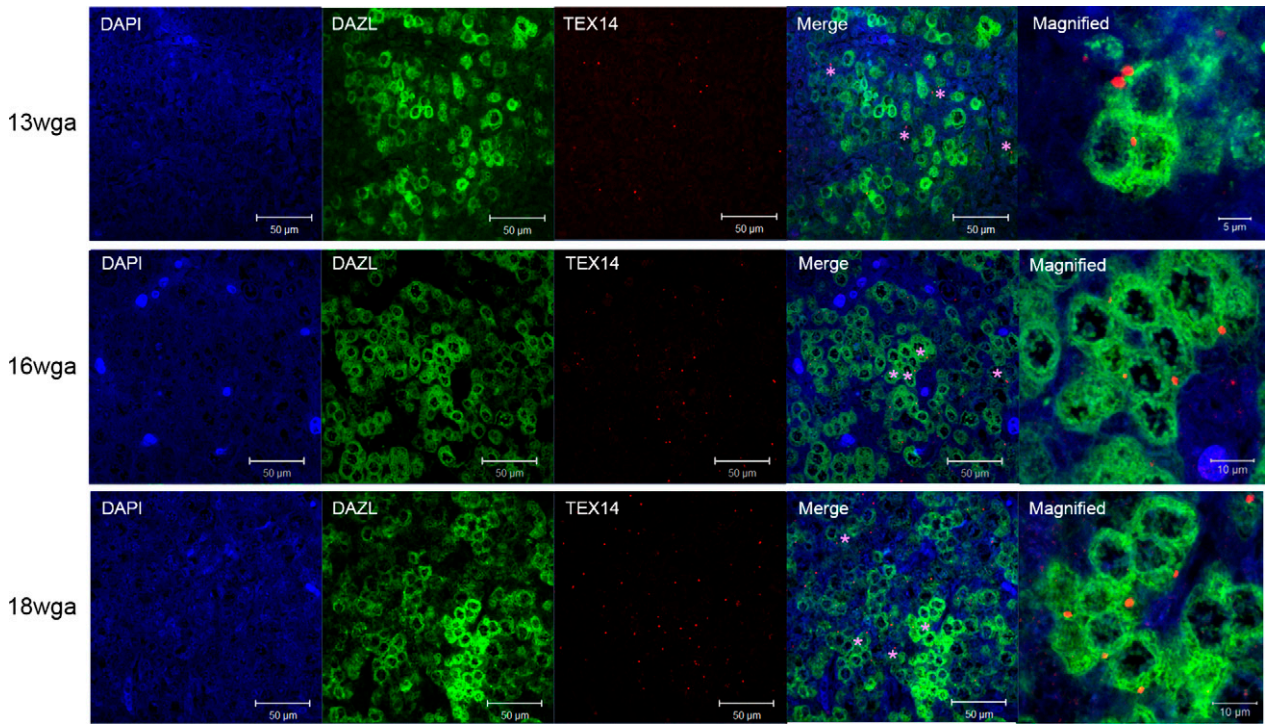

Figure 6. TEX14 is coexpressed with DAZL across gestation in the human fetal ovary. Representative images of coimmunostaining for TEX14 (red) and DAZL (green) across gestation in the human fetal ovary. In merge image, TEX14 foci in the cytoplasm of DAZL-positive germ cells in germ cell nest structures are denoted with a purple asterisk. Scale bars: 50 μM; magnified image, 5 μM (13 wga) and 10 μM (16 and 18 wga).

only, suggesting apoptosis may have occurred during germ cell nest breakdown. Consistent with this, Dazl has been shown to inhibit the translation of key proapoptotic caspases, *Caspase 2*, *7*, and *9* (44). These data suggest that potentially a complete ablation of Dazl expression is required to induce widespread early apoptosis in germ cells, or more likely, the timing of when Dazl expression is reduced is critical. In this model, we are manipulating Dazl expression at e13.5, when germ cells have already lost their pluripotency and are committed to an oogonial fate (45).

Although Dazl hypomorph ovaries had fewer follicles in total, the majority of follicles observed were primordial stage, and these PMFs had a smaller oocyte nuclear diameter compared with controls at both doses of siRNA, which persisted up to d 14 of culture in the 15 nM dose (the equivalent of ~postnatal d 5–6). Interestingly, Dazl$^{+/-}$ mice have no difference in follicle

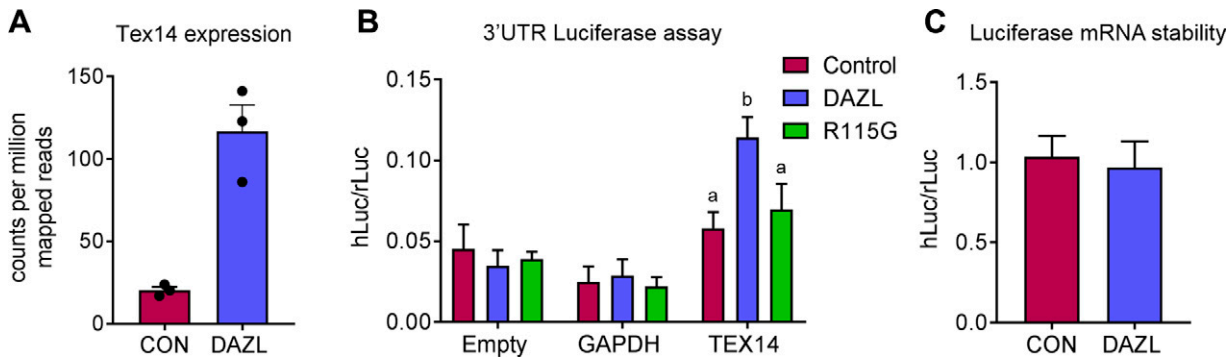

Figure 7. DAZL binds the 3′UTR of TEX14 and stimulates translation. *A*) Graph displays counts per million mapped reads of TEX14 taken from DAZL RNA-immunoprecipitation and sequencing experiment described in Rosario *et al.* (24). Circles depict data from individual experiments. Error bars indicate means ± SE. *B*) 3′UTR-luciferase reporter activity in the presence of empty vector control (magenta bar), DAZL (blue bar), or R115G DAZL mutant (green bar). Firefly luciferase signals were normalized to *Renilla* luciferase signals. Error bars indicate means ± SE; $n = 4$. $P = 0.027$, Dunns multiple comparison test. *C*) TEX14 3′UTR-luciferase mRNA expression in the presence or absence of DAZL. Expression was analyzed 48 h after transfection. Firefly luciferase mRNA expression was normalized to *Renilla* luciferase mRNA expression. Con, control; GAPDH, glyceraldehyde 3-phosphate dehydrogenase. Error bars indicate means ± SE; $n = 4$ for each group. hLuc, humanised firefly luciferase; rLuc, *Renilla* luciferase.

number or follicle stage at postnatal d 21 (16). We also found that there was an increased number of germ cells still in nest structures in Dazl hypomorph ovaries. Combined with the follicle data, these lines of evidence suggest that the knockdown of Dazl delayed germ cell maturation, and as a result, more germ cells were still in nests and had not yet formed PMFs. Importantly, we have demonstrated that this siRNA does not have any off-target effects in reducing the expression of the closely related RNA-binding protein, Boll. Boll is the ancestral member of the DAZ family of RNA-binding proteins, and functional studies have shown that Bol homologs are essential for progression beyond pachytene of prophase I in *Caenorhabditis elegans* females and *Drosophila* males (46, 47). We have previously reported that Dazl and Boll are coexpressed in the mouse fetal germline (48), and given the possibility of functional redundancy between these 2 proteins, it was important that Boll expression was unaffected by Dazl knockdown, allowing us to attribute any phenotypic effects we observed solely to Dazl.

In addition to enabling germ cell response to the meiosis-inducing signal retinoic acid, Dazl also regulates the translation of many mRNAs that have critical roles during prophase [see Rosario *et al*. (38) for a review on mRNA targets of DAZL]. Although Sycp3 is a Dazl target (22), there is no evidence that suggests that Dazl stimulates the translation of Sycp3 in meiotic oocytes to the extent that it is required for Sycp3 function. Sycp3 is also expressed and present in Dazl null oocytes (12); therefore, it was used in combination with Sycp1 to monitor synapsis in this model. We hypothesized that the knockdown of Dazl interfered with the progression of prophase I in our cultured ovaries, subsequently delaying germ cell nest breakdown and PMF assembly. However, detailed cytologic analysis of the synaptonemal complex in oocytes from cultured ovaries revealed that, following Dazl knockdown, the axial element is able to form normally, and homologous chromosomes pair and synapse successfully in pachytene. Furthermore, the dynamics of progression into the late stages of meiotic prophase I, from pachytene, through the process of desynapsis and synaptonemal complex disassembly into late-diplotene and dictyate, were unaltered following Dazl knockdown. Given there was a significant difference in PMF formation, with no changes in meiotic progression, it appears that germ cell maturation and meiosis have been uncoupled in Dazl hypomorph oocytes. Comparably, stimulated by retinoic acid gene 8 (Stra8)-deficient ovarian germ cells grow and differentiate into oocyte-like cells that form follicles and are capable of fertilization in the absence of premeiotic chromosomal replication, sister chromatid cohesion, synapsis, or recombination, thus demonstrating that oocyte growth and differentiation are genetically dissociable from the chromosomal events of prophase I (49). Alternatively, it is possible that despite Dazl being involved in the regulation of many key factors in meiotic prophase, these relationships are either dispensable, timing dependent, or are not sufficiently perturbed in this knockdown model to yield a detectable change in the capacity of oocytes to progress through meiotic prophase.

Tex14 is an essential component of male and female intercellular bridges (25), and *Tex14* mRNA has previously been reported to coprecipitate with Dazl from rat and mouse testis extracts (22). In addition, RNA immunoprecipitation and subsequent sequencing using human fetal ovarian tissue identified *TEX14* as a putative DAZL mRNA target (24). It appears there is a conserved consensus Dazl binding site in the 3′UTRs of Tex14 from these species (50); however, there have been no further investigations or confirmatory experiments carried out exploring the relationship between Tex14 and Dazl. Tex14 localizes to germ cell intercellular bridges, and in the absence of Tex14, these bridges cannot be observed by electron microscopy (51). Dazl hypomorph ovaries had significantly fewer Tex14 foci, and these foci were smaller than those found in scramble control–cultured ovaries. Moreover, this reduction in Tex14 protein expression was not a result of altered mRNA levels, which indicates that this difference is the result of impaired posttranscriptional regulation. The present data using translational assays confirm for the first time that *TEX14* is indeed a DAZL mRNA target, and we have shown the colocalization of TEX14 foci and DAZL to the cytoplasm of germ cells found in nest structures in the human fetal ovary. Therefore, we suggest that the reduction of Dazl expression in our hypomorph model has caused a reduction in Tex14 expression with reduced and abnormal intercellular bridge function, which has affected the structure and function of germ cell nests. Consequently, these nests are unable to break down efficiently and then form PMFs, and as a result, many germ cells are lost. This may also be the basis for the oocytes within Dazl hypomorph PMFs being smaller; the intercellular bridges are thought to contribute to cytoplasmic and organelle movement between oocytes prior to nest breakdown, into those oocytes destined to survive and form follicles (6, 8). Supporting the importance of Tex14 in mediating this Dazl hypomorph phenotype, the ovaries of Tex14 null mice have roughly half the initial oocyte pool compared with controls, despite there being similar numbers of germ cells in control and $Tex14^{-/-}$ ovaries in the genital ridge at e11.5 and just before germ cell nest breakdown at e18.5 (52).

The RNA-binding protein Dazl is well established as an important regulator of germ cell development; however, in this work, we have created a model using siRNA and mouse fetal ovary culture, which allowed us to study Dazl function in germ cells once meiosis is underway. Here, we have demonstrated a novel role for Dazl function during germ cell maturation and PMF formation, and using translational assays, we have confirmed the role of Dazl in the regulation of Tex14 expression. We suggest through the translational regulation of Tex14, the absence of Dazl has a significant impact on the breakdown of germ cell nests and subsequent assembly of PMFs. FJ

ACKNOWLEDGMENTS

The authors thank Anne Saunderson and the staff of the Bruntsfield Suite, Royal Infirmary of Edinburgh, for recruitment,

and to members of the Shared University Research Facilities (SuRF) at the University of Edinburgh (*https://surf.ed.ac.uk*), especially Mike Millar, for assistance. The authors' work in this field was support by grants from the Medical Research Council (MRC; G1100357 to R.A.A., MR/N022556/1 to the MRC Centre for Reproductive Health, and an intramural programme grant to I.R.A.) and the Biotechnology and Biological Sciences Research Council (BB/R015635/1 to R.A.A., R.R., and I.R.A.). The authors declare no conflicts of interest.

AUTHOR CONTRIBUTIONS

R. Rosario, J. H. Crichton, I. R. Adams, and R. A. Anderson designed the experiments; R. Rosario, J. H. Crichton, and H. L. Stewart carried out experiments; R. Rosario drafted the manuscript; and all authors contributed to data interpretation, editing of the manuscript, and its final approval.

REFERENCES

1. Witschi, E. (1948) Migration of germ cells of human embryos from the yolk sac to the primitive gonadal folds. *Contrib. Embryol. Carnegie Inst.* **32**, 67–80
2. Ginsburg, M., Snow, M. H., and McLaren, A. (1990) Primordial germ cells in the mouse embryo during gastrulation. *Development* **110**, 521–528
3. Lei, L., and Spradling, A. C. (2013) Mouse primordial germ cells produce cysts that partially fragment prior to meiosis. *Development* **140**, 2075–2081
4. Pepling, M. E., de Cuevas, M., and Spradling, A. C. (1999) Germline cysts: a conserved phase of germ cell development? *Trends Cell Biol.* **9**, 257–262
5. De Cuevas, M., Lilly, M. A., and Spradling, A. C. (1997) Germline cyst formation in Drosophila. *Annu. Rev. Genet.* **31**, 405–428
6. Tingen, C., Kim, A., and Woodruff, T. K. (2009) The primordial pool of follicles and nest breakdown in mammalian ovaries. *Mol. Hum. Reprod.* **15**, 795–803
7. Pepling, M. E., and Spradling, A. C. (2001) Mouse ovarian germ cell cysts undergo programmed breakdown to form primordial follicles. *Dev. Biol.* **234**, 339–351
8. Lei, L., and Spradling, A. C. (2016) Mouse oocytes differentiate through organelle enrichment from sister cyst germ cells. *Science* **352**, 95–99
9. Pepling, M. E., and Spradling, A. C. (1998) Female mouse germ cells form synchronously dividing cysts. *Development* **125**, 3323–3328
10. Gondos, B., Bhiraleus, P., and Hobel, C. J. (1971) Ultrastructural observations on germ cells in human fetal ovaries. *Am. J. Obstet. Gynecol.* **110**, 644–652
11. Ruggiu, M., Speed, R., Taggart, M., McKay, S. J., Kilanowski, F., Saunders, P., Dorin, J., and Cooke, H. J. (1997) The mouse Dazla gene encodes a cytoplasmic protein essential for gametogenesis. *Nature* **389**, 73–77
12. Saunders, P. T., Turner, J. M., Ruggiu, M., Taggart, M., Burgoyne, P. S., Elliott, D., and Cooke, H. J. (2003) Absence of mDazl produces a final block on germ cell development at meiosis. *Reproduction* **126**, 589–597
13. Lin, Y., and Page, D. C. (2005) Dazl deficiency leads to embryonic arrest of germ cell development in XY C57BL/6 mice. *Dev. Biol.* **288**, 309–316
14. Schrans-Stassen, B. H., Saunders, P. T., Cooke, H. J., and de Rooij, D. G. (2001) Nature of the spermatogenic arrest in Dazl -/- mice. *Biol. Reprod.* **65**, 771–776
15. Haston, K. M., Tung, J. Y., and Reijo Pera, R. A. (2009) Dazl functions in maintenance of pluripotency and genetic and epigenetic programs of differentiation in mouse primordial germ cells in vivo and in vitro. *PLoS One* **4**, e5654
16. McNeilly, J. R., Watson, E. A., White, Y. A., Murray, A. A., Spears, N., and McNeilly, A. S. (2011) Decreased oocyte DAZL expression in mice results in increased litter size by modulating follicle-stimulating hormone-induced follicular growth. *Biol. Reprod.* **85**, 584–593
17. Chen, J., Melton, C., Suh, N., Oh, J. S., Horner, K., Xie, F., Sette, C., Blelloch, R., and Conti, M. (2011) Genome-wide analysis of translation reveals a critical role for deleted in azoospermia-like (Dazl) at the oocyte-to-zygote transition. *Genes Dev.* **25**, 755–766
18. Fukuda, K., Masuda, A., Naka, T., Suzuki, A., Kato, Y., and Saga, Y. (2018) Requirement of the 3′-UTR-dependent suppression of DAZL in oocytes for pre-implantation mouse development. *PLoS Genet.* **14**, e1007436
19. Tsui, S., Dai, T., Warren, S. T., Salido, E. C., and Yen, P. H. (2000) Association of the mouse infertility factor DAZL1 with actively translating polyribosomes. *Biol. Reprod.* **62**, 1655–1660
20. Collier, B., Gorgoni, B., Loveridge, C., Cooke, H. J., and Gray, N. K. (2005) The DAZL family proteins are PABP-binding proteins that regulate translation in germ cells. *EMBO J.* **24**, 2656–2666
21. Reynolds, N., Collier, B., Bingham, V., Gray, N. K., and Cooke, H. J. (2007) Translation of the synaptonemal complex component Sycp3 is enhanced in vivo by the germ cell specific regulator Dazl. *RNA* **13**, 974–981
22. Reynolds, N., Collier, B., Maratou, K., Bingham, V., Speed, R. M., Taggart, M., Semple, C. A., Gray, N. K., and Cooke, H. J. (2005) Dazl binds in vivo to specific transcripts and can regulate the pre-meiotic translation of Mvh in germ cells. *Hum. Mol. Genet.* **14**, 3899–3909
23. Welling, M., Chen, H. H., Muñoz, J., Musheev, M. U., Kester, L., Junker, J. P., Mischerikow, N., Arbab, M., Kuijk, E., Silberstein, L., Kharchenko, P. V., Geens, M., Niehrs, C., van de Velde, H., van Oudenaarden, A., Heck, A. J., and Geijsen, N. (2015) DAZL regulates Tet1 translation in murine embryonic stem cells. *EMBO Rep.* **16**, 791–802
24. Rosario, R., Smith, R. W., Adams, I. R., and Anderson, R. A. (2017) RNA immunoprecipitation identifies novel targets of DAZL in human foetal ovary. *Mol. Hum. Reprod.* **23**, 177–186
25. Greenbaum, M. P., Iwamori, T., Buchold, G. M., and Matzuk, M. M. (2011) Germ cell intercellular bridges. *Cold Spring Harb. Perspect. Biol.* **3**, a005850
26. Tung, J. Y., Rosen, M. P., Nelson, L. M., Turek, P. J., Witte, J. S., Cramer, D. W., Cedars, M. I., and Reijo-Pera, R. A. (2006) Novel missense mutations of the Deleted-in-AZoospermia-Like (DAZL) gene in infertile women and men. *Reprod. Biol. Endocrinol.* **4**, 40
27. Bartoloni, L., Cazzadore, C., Ferlin, A., Garolla, A., and Foresta, C. (2004) Lack of the T54A polymorphism of the DAZL gene in infertile Italian patients. *Mol. Hum. Reprod.* **10**, 613–615
28. Zerbetto, I., Gromoll, J., Luisi, S., Reis, F. M., Nieschlag, E., Simoni, M., and Petraglia, F. (2008) Follicle-stimulating hormone receptor and DAZL gene polymorphisms do not affect the age of menopause. *Fertil. Steril.* **90**, 2264–2268
29. Childs, A. J., and Anderson, R. A. (2012) Experimental approaches to the study of human primordial germ cells. *Methods Mol. Biol.* **825**, 199–210
30. Ramakers, C., Ruijter, J. M., Deprez, R. H., and Moorman, A. F. (2003) Assumption-free analysis of quantitative real-time polymerase chain reaction (PCR) data. *Neurosci. Lett.* **339**, 62–66
31. Van den Bergen, J. A., Miles, D. C., Sinclair, A. H., and Western, P. S. (2009) Normalizing gene expression levels in mouse fetal germ cells. *Biol. Reprod.* **81**, 362–370
32. Livak, K. J., and Schmittgen, T. D. (2001) Analysis of relative gene expression data using real-time quantitative PCR and the 2(-Delta Delta C(T)) Method. *Methods* **25**, 402–408
33. Vandesompele, J., De Preter, K., Pattyn, F., Poppe, B., Van Roy, N., De Paepe, A., and Speleman, F. (2002) Accurate normalization of real-time quantitative RT-PCR data by geometric averaging of multiple internal control genes. *Genome Biol.* **3**, RESEARCH0034
34. Peters, A. H., Plug, A. W., van Vugt, M. J., and de Boer, P. (1997) A drying-down technique for the spreading of mammalian meiocytes from the male and female germline. *Chromosome Res.* **5**, 66–68
35. Abercrombie, M. (1946) Estimation of nuclear population from microtome sections. *Anat. Rec.* **94**, 239–247
36. Stefansdottir, A., Johnston, Z. C., Powles-Glover, N., Anderson, R. A., Adams, I. R., and Spears, N. (2016) Etoposide damages female germ cells in the developing ovary. *BMC Cancer* **16**, 482
37. Lin, Y., Gill, M. E., Koubova, J., and Page, D. C. (2008) Germ cell-intrinsic and -extrinsic factors govern meiotic initiation in mouse embryos. *Science* **322**, 1685–1687
38. Rosario, R., Adams, I. R., and Anderson, R. A. (2016) Is there a role for DAZL in human female fertility? *Mol. Hum. Reprod.* **22**, 377–383

39. Houmard, B., Small, C., Yang, L., Naluai-Cecchini, T., Cheng, E., Hassold, T., and Griswold, M. (2009) Global gene expression in the human fetal testis and ovary. *Biol. Reprod.* **81**, 438–443
40. Anderson, R. A., Fulton, N., Cowan, G., Coutts, S., and Saunders, P. T. (2007) Conserved and divergent patterns of expression of DAZL, VASA and OCT4 in the germ cells of the human fetal ovary and testis. *BMC Dev. Biol.* **7**, 136
41. Tung, J. Y., Rosen, M. P., Nelson, L. M., Turek, P. J., Witte, J. S., Cramer, D. W., Cedars, M. I., and Pera, R. A. (2006) Variants in Deleted in AZoospermia-Like (DAZL) are correlated with reproductive parameters in men and women. *Hum. Genet.* **118**, 730–740
42. Jenkins, H. T., Malkova, B., and Edwards, T. A. (2011) Kinked β-strands mediate high-affinity recognition of mRNA targets by the germ-cell regulator DAZL. *Proc. Natl. Acad. Sci. USA* **108**, 18266–18271
43. Feng, C. W., Bowles, J., and Koopman, P. (2014) Control of mammalian germ cell entry into meiosis. *Mol. Cell. Endocrinol.* **382**, 488–497
44. Chen, H. H., Welling, M., Bloch, D. B., Muñoz, J., Mientjes, E., Chen, X., Tramp, C., Wu, J., Yabuuchi, A., Chou, Y. F., Buecker, C., Krainer, A., Willemsen, R., Heck, A. J., and Geijsen, N. (2014) DAZL limits pluripotency, differentiation, and apoptosis in developing primordial germ cells. *Stem Cell Reports* **3**, 892–904
45. Adams, I. R., and McLaren, A. (2002) Sexually dimorphic development of mouse primordial germ cells: switching from oogenesis to spermatogenesis. *Development* **129**, 1155–1164
46. Eberhart, C. G., Maines, J. Z., and Wasserman, S. A. (1996) Meiotic cell cycle requirement for a fly homologue of human Deleted in Azoospermia. *Nature* **381**, 783–785
47. Karashima, T., Sugimoto, A., and Yamamoto, M. (2000) Caenorhabditis elegans homologue of the human azoospermia factor DAZ is required for oogenesis but not for spermatogenesis. *Development* **127**, 1069–1079
48. He, J., Stewart, K., Kinnell, H. L., Anderson, R. A., and Childs, A. J. (2013) A developmental stage-specific switch from DAZL to BOLL occurs during fetal oogenesis in humans, but not mice. *PLoS One* **8**, e73996; erratum: 10, e0136009
49. Dokshin, G. A., Baltus, A. E., Eppig, J. J., and Page, D. C. (2013) Oocyte differentiation is genetically dissociable from meiosis in mice. *Nat. Genet.* **45**, 877–883
50. Venables, J. P., Ruggiu, M., and Cooke, H. J. (2001) The RNA-binding specificity of the mouse Dazl protein. *Nucleic Acids Res.* **29**, 2479–2483
51. Greenbaum, M. P., Yan, W., Wu, M. H., Lin, Y. N., Agno, J. E., Sharma, M., Braun, R. E., Rajkovic, A., and Matzuk, M. M. (2006) TEX14 is essential for intercellular bridges and fertility in male mice. *Proc. Natl. Acad. Sci. USA* **103**, 4982–4987
52. Greenbaum, M. P., Iwamori, N., Agno, J. E., and Matzuk, M. M. (2009) Mouse TEX14 is required for embryonic germ cell intercellular bridges but not female fertility. *Biol. Reprod.* **80**, 449–457

Received for publication May 17, 2019.
Accepted for publication September 17, 2019.